Variable Optical Power Splitter with Field-Induced Waveguides in Liquid Crystals in Paranematic Phase

Conference Paper · March 2014

DOI: 10.1364/OFC.2014.Th1A.7

4 authors, including:

Florenta Costache
Fraunhofer Institute for Photonic Microsystems IPMS
53 PUBLICATIONS **1,239** CITATIONS

Variable Optical Power Splitter with Field-Induced Waveguides in Liquid Crystals in Paranematic Phase

F. Costache, H. Hartwig, K. Bornhorst, and M. Blasl
Fraunhofer Institute for Photonic Microsystems, Maria-Reiche-Str. 2, 01109 Dresden, Germany
florenta.costache@ipms.fraunhofer.de

Abstract: A novel 1×2 variable optical power splitter based on field-induced waveguides in paranematic phase liquid crystals is reported. Continuously, voltage adjustable splitting with sub-microsecond response time is demonstrated on a device fabricated on silicon backplane.
OCIS codes: (230.7370) Waveguides; (160.3710) Liquid crystals; (130.4815) Optical switching devices.

1. Introduction

Optical power splitters (OPSs) ensure the functions of splitting and combining of optical signals in optical telecommunication networks. By employing OPSs with variable optical splitting ratio, the optical power can be flexibly and dynamically redistributed, in real-time, in the entire network, this providing advantages such as improvement in network efficiency, scalability and reliability. The existing OPSs concepts are mainly passive and only a few variable OPSs designs have been reported such as OPSs using the capability of opto-very large scale integrated (Opto-VLSI) technology [1], OPSs based on slot waveguides [2], or OPSs based on polarization signal processing with micro-optical components [3]. Although essential demands for optical communication applications are met, these structures still have limitations from the viewpoints of integration, scalability and reliability.

In this paper, we report on a novel concept of integrated variable OPS based on field-induced waveguides (FIWs). Such waveguides can be induced by locally applying electrical fields across a waveguide sandwich with a core layer made of an electro-optical (EO) material. As core EO materials, these waveguides employ special liquid crystals heated towards their nematic to isotropic phase (N-I) transition. Specifically this transition is also known as the nematic to paranematic (N-PN) transition in the presence of electrical fields [4]. In this particular phase, liquid crystals can exhibit very useful properties for FIWs, such as large EO Kerr constants, very good transparency from visible to infrared range and sub-microsecond response times [5]. The characteristics of a variable, dynamic OPS device based on this concept and fabricated by means of silicon wafer micro-machining are here presented.

2. Liquid crystals in paranematic phase

Several thermotropic liquid crystals such as for example 5CB could be employed as core EO materials for the FIWs. In order to design the waveguide, we needed to first determine the temperature range in the vicinity of the N-PN transition, at which the material exhibits large EO Kerr constants K_0, and where optimal field induced anisotropies Δn are expected. We could extract K_0 from the expression $\Delta n = \lambda K_0 E^2/(T\text{-}T^*)$, with λ the wavelength of light, E the electric field, and T^* a so-called transition temperature, which was derived from the Landau - de Gennes theory for liquid crystals [6] to describe the EO Kerr effect for liquid crystals at this transition.

The temperature dependent field induced anisotropy Δn was obtained by analyzing the thin film interference in a layer of liquid crystal enclosed in a cell. The cell was maintained at a temperature just above the liquid crystal's N-PN transition T_{NI} (here, 34.7 °C).

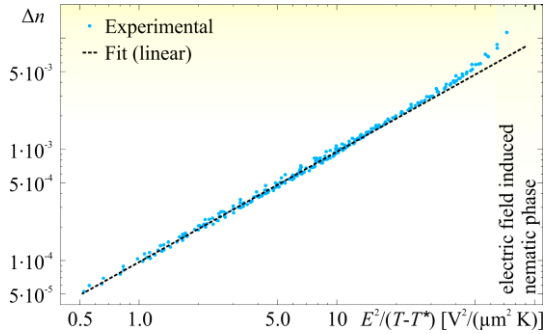

Fig. 1. Induced birefringence as a function of both quadratic electric field and temperature (T* = 34.0 °C). The deviation from the linear behavior is due to higher order terms of Δn dependence on electric field. At high electric fields the induced nematic phase sets in [4].

978-1-55752-993-0/14/$31.00 ©2014 Optical Society of America

Fig. 1 shows the results for the Δn for 5CB as a function of both quadratic electric field and temperature. For these measurements we varied the temperature and the electric field within these intervals: T = (34.8 - 41) °C and E = (0 - ±7.7) V/µm. From the linear fit on the experimental data, we could obtain a Kerr constant of about $K_0 = 1.5 \cdot 10^{-10}$ Km/V^2. The achieved Δn at the order of 10^{-3} indicates that 5CB in this particular phase is a valid core material for FIWs. It should be mentioned that these measurements were carried out at λ = 632.8 nm. Nonetheless, for λ = 1550 nm, Δn and K_0 are expected to be of the same order of magnitude.

3. Device design and fabrication

The FIW geometry was designed using a finite element simulation method (FEM) for TM polarized, single mode operation at 1550 nm telecom wavelength. This waveguide geometry, which extends to 1 cm in length, is presented in cross section in Fig. 2(a).

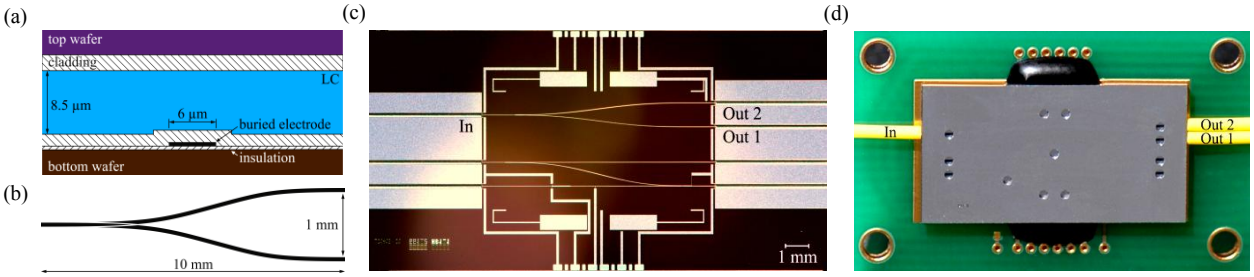

Fig. 2: (a) FIW principle geometry in cross section; (b) 1 × 2 variable OPS's bottom Y-junction electrode geometry; (c) Image of processed bottom part of the OPS chip. (This includes, beside the electrodes for the OPS, also electrodes for straight waveguides); (d) 1 × 2 variable OPS chip assembly, mounted on a temperature stabilizing printed circuit board.

As schematically shown in Fig. 2(b), the waveguide structure of the 1 × 2 variable OPS, essentially includes three bottom electrodes, designed as a symmetric Y-junction, and a counter top electrode (i.e. the top wafer in Fig. 2(a)). Each of the bottom electrodes can be individually electrically addressed. Electrical fields applied between top and bottom electrodes and across the liquid crystal layer could therefore enable a variable, continuous, and controlled adjustment of the signal intensity on the two output ports.

A liquid crystal cell chip comprising this OPS geometry was fabricated on silicon wafers in a standard silicon micro-fabrication line. The chip consists of two processed silicon substrates forming the bottom and the top parts of the chip, each including structured electrodes, as indicated above, and low refractive index claddings made of SiO_x. Fig. 2(c) shows, for example, an image of the bottom part of the chip. In particular, for the 1 × 2 OPS design, the bottom wafer includes structured aluminum electrodes and V-grooves, etched in silicon, for the precise alignment of fiber to waveguide. The top wafer was structured using lithography processes to contain a cavity for the liquid crystals. Here, for the single mode operation, the cavity height was set to 8.5 µm. For completing the chip assembly, the wafers were bonded together, fibers were placed in the V-grooves and the cavity was then filled with liquid crystals. The chip assembly is presented in Fig. 2(d).

4. Device characterization

The device characterization included measurements of optical transmission for the variable OPS device set to various splitting ratios, from which insertion loss and attenuation range could be derived, as well as measurements of its temporal dynamics (Fig. 3). For these measurements, light from a coherent TM polarized light source at 1550 nm wavelength was coupled into the device through a single mode polarization maintaining fiber. The output signal was captured using a standard single mode fiber, directly coupled to one of the output ports of the splitter.

As indicated in the inset from Fig. 3(a), the splitter has three individually addressable electrodes, namely 'In', 'Out 1', and 'Out 2', which correspond to the OPS's input, output 1 and output 2 ports, respectively. For characterization purposes, 'In' and 'Out 1', where held at the same but variable voltage denoted as U_1, while on 'Out 2' a variable voltage U_2 was applied. In this way, by taking into consideration the device symmetry, the monitoring of only one output was sufficient to determine the total transmission characteristics of the variable OPS. The relative transmission at the port output 1 was therefore recorded with a photodiode for sets of voltages (U_1, U_2) with both U_1 and U_2 being varied between 0 V to U_{max}, where U_{max} = 150 V in our setup. The obtained data were represented as a function of the applied voltages as shown in Fig. 3(a). To ease interpretation of this plot, subsets of data from Fig. 3(a) are presented in Fig. 3(b) and Fig. 3(c). Several distinct parameters of the variable OPS can be derived from these plots. For instance, the maximum insertion loss on each channel, which stems from loss at fiber-to-chip coupling, propagation loss, and loss at the Y-junction, amounts to around 5 dB (also indicated in Fig. 3(b)). Further,

both optical paths could be attenuated each by around 30 dB, when both U_1 and U_2 are set below $0.6 \cdot U_{max}$ (see also Fig. 3(b)), while for specific sets of U_1 and U_2 voltages it is possible to set the splitter to any other splitting ratios and attenuation. The 3 dB power splitting ratio is achieved when both U_1 and U_2 equal U_{max} (as indicated in Fig. 3(c)). Particularly in Fig. 3(b) the plot presents the variable attenuation on one of the channels (Out 1) and Fig. 3(c) presents the variable power splitting on the two channels (Out 1 and Out 2) obtained by varying the voltage on the corresponding electrodes as indicated.

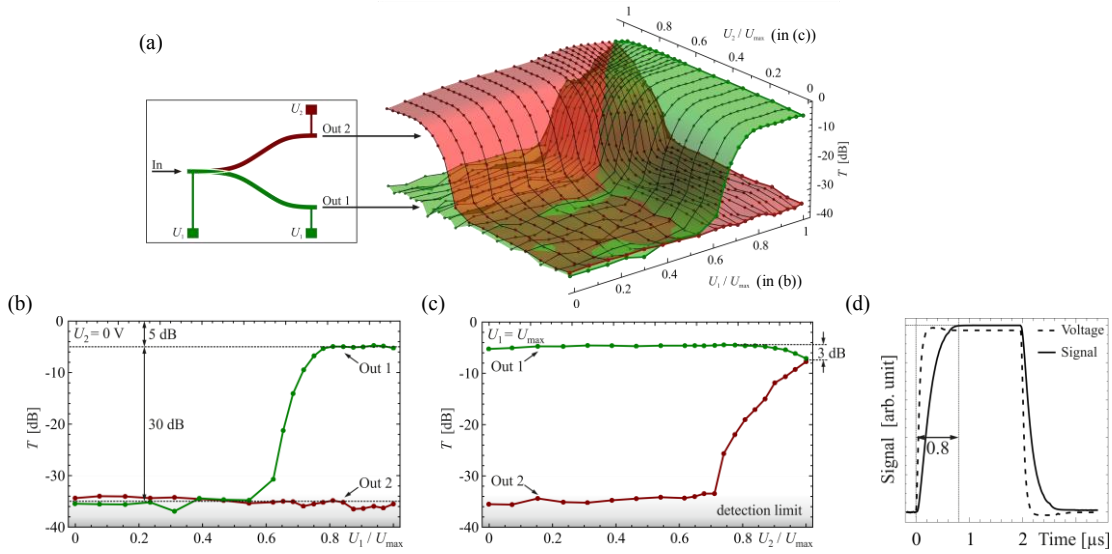

Fig. 3: (a) Transmission vs. applied voltage measured on the two channels of the liquid crystal OPS chip (U_1 voltage on the electrodes marked with green, U_2 voltage applied on the electrode marked with red); (b, c) Variable attenuation and variable power splitting (data from (a)); (d) Measured response time.

Furthermore, by employing a pulsed electric driving signal and recording the corresponding optical output, a response (switching) time of less than a microsecond could be estimated (see Fig. 3(d)).

5. Conclusions

An integrated 1×2 dynamic optical power splitter based on field induced waveguides in liquid crystals in paranematic phase was designed using FEM simulation and fabricated by means of silicon bulk micro-machining processes. We show that this concept enables the possibility of sub-microsecond, dynamic, continuously voltage controlled adjustment of the output signal on the two ports. Essentially, by adjusting the voltage on the electrodes corresponding to the two output ports, continuous optical power splitting and attenuation ratios from 0 dB to 30 dB can be obtained.

6. Acknowledgements

Funding from the Fraunhofer Internal Programs under Grant No. Attract 692123 is greatly acknowledged. Further developments are supported by the German Federal Ministry of Education and Research (BMBF) within the funding program Photonics Research Germany, Contract No. 13N12442.

7. References

[1] H.A.B. Mustafa et al., "A 1x2 adaptive optical splitter based on Opto-VLSI processor", In: High-Capacity Optical Networks and Enabling Technologies (HONET), IEEE, 200 (2010).

[2] Zheng et al., "Variable optical power splitter based on slot waveguide", In: Asia Communications and Photonics, International Society for Optics and Photonics, 76301D (2009).

[3] Z. Yun et al., "A 1 x 2 Variable Optical Power Splitter Development", Journal of Lightwave Technology **24**, 1566 (2006).

[4] E.I. Rjumtse et al., "Electric field effect on the nematic-isotropic phase transition", Liquid Crystals **18**, 87 (1995)

[5] R. Yamamota et al., "The Kerr constants and relaxation times in the isotropic phase of nematic homologous series", Phys. Lett. A **69,** 276 (1978).

[6] I.C. Khoo, *Liquid Crystals: Physical Properties and Nonlinear Optical Phenomena*, Wiley Interscience, New York, (2007).